Journal of Ovonic Research Vol. 17, No. 6, November - December 2021, p. 499 - 507

The role of Co in doping ZnO nano-particles in enhancement the structural, optical and magnetic properties for spintronics

A. Abu El-Fadl[a], Ragaa S.Mahmoud[a], A. A. Abu-Sehly[a], El Sayed Yousef[b,c],
E. R. Shaaban[d], Mohamed N. Abd-el Salam[e,*]
[a] *Physics Department, Faculty of Science, Assiut University, Assiut 71516, Egypt*
[b] *Physics Department, Faculty of Science, King Khalid University, P.O. Box 9004, Abha, Saudi Arabia*
[c] *Research Center for Advanced Materials Science (RCAMS), King Khalid University, Abha 61413, P.O. Box 9004, Saudi Arabia*
[d] *Physics Department, Faculty of Science, Al-Azhar University, Assiut, 71542, Egypt*
[e] *Higher Institute for Engineering and Technology, El-Minya 61768, Egypt*

$Zn_{1-x}Co_xO$ ($0 \leq x \leq 0.10$) nano-particles were fabricated successfully via ball milling procedure. The influence of [Co]/[Zn] on the properties of nano-particles was examined employing X-ray diffraction, the energy dispersion of the X-ray (EDX), Scan Electron Microscope (SEM), these measurements exhibit the growth hexagonal wurtzite crystal phase $Zn_{1-x}Co_xO$ nano-particles with the successfully incorporation of Co^{+2} ions in the ZnO lattice. The optical characterization investigated utilizing Ultraviolet-Visible (UV) absorption spectroscopy for $Zn_{1-x}Co_xO$ nano-particles refers to a red-shift in the optical bandgap with increasing Co ion inside ZnO matrix, this result confirm the bandgap is considerably narrowed with increasing Co ratio. The measurements of magnetization applying vibrating sample magnetometer illustrated a hysteresis loop in Co-doped ZnO nano-particles. Thanks to the variation values of bandgap E_g^{opt} and magnetic measurements of ZnO nano-particles doped Co% plays a major role for selective coatings of optoelectronics; use as antireflective coating materials, and fabrication of opto-electronic devices.

(Received July 25, 2021; Accepted November 3, 2021)

Keywords: $Zn_{1-x}Co_xO$ nanoparticles, Ball milling method, Structural parameters, Optical characterization, Hysteresis loop

1. Introduction

Zinc oxide nano-particles are promising semiconductors due to their interesting chemical and physical properties. Owing to a wide direct bandgap (3.2 - 3.4 ev) and a large binding energy of exciton (60 meV), these characteristics make ZnO nano-particles compound are one of the ideal materials for short-wavelength opto-electronic and nano-electronic devices[1-4]. Furthermore, ZnO nano-particles have piezoelectric, pyroelectric and photo-corrosion stability characteristics makes them an appealing material for sensors and energy producers [5, 6]. More than, ZnO has been proposed for spintronics and other scientific uses as biotechnology, inmedicinal applications and it is also, one of the materials that may be used with carbon paste electrodes for utilizing in electro-chemical sensors [7-10]

Doping in the host matrix nano-particles ZnO, such as manganese,(Mn), copper,(Cu), cobalt,(Co), vanadium,(V), Silver,(Ag), and others, plays an essential part in enhancing the physical/chemical characteristics of developed research and applications of technology [11-14]. Cobalt,(Co) has emerged as the better material for doping into the transition metals on account of its dis-solvable nature in the ZnO lattice and Co possessing a near ionic radius (0.58 Å) to Zn (0.60 Å), also, Co^{2+} owns five spins in the half/filled 3d shell, which leads to raises magnetization levels and the highest value of dipole moment 3 μB per Co ion.

---

[*] Corresponding author: moha_nabile2010@yahoo.com

Additionally, Co-doped ZnO has been also considered a more appropriate candidate as one of the first diluted magnetic semiconductor (DMS) systems to be studied [15]. In fact, ZnO considered is a new visible-light photo-catalyst with major potential[16]. that can maximize solar energy for the photocatalytic degradation of pollutants compared with traditional photo-catalysts, such as TiO_2 [17, 18] and SnO_2 [19]systems. In addition, to the crystal structure a perfect photocatalyst should likewise possess a suitable absorption band and a high specific surface region. As an example, the former property can be accomplished by tailoring the optical bandgap by doping [15, 20, 21]. Furthermore, dilute magnetic semiconductor (DMS) materials have piqued the interest of researchers in recent years due to the combination of magnetic and semiconductor characteristics in a single material. Some of the potential applications offered by DMS materials are spintronics that exploit both the electron charge connected with the intrinsic spin of the electron[22]. Physical properties, such as bandgap energy or magnetism, are now not only a function of particle size but also of the level of doping. Therefore, nanometer-sized magnetic semiconductor ordered arrays are interesting materials for modern devices in magnetic or spin electronics[22]. It is well known that the Co doped ZnO as a nano particles are significantly dilute semiconductor and prepared by varies methods such as solution combustion synthesis[23], chemical co-precipitation method [24, 25], a wet chemical method[26], as well as several other methods. Ball milling [21] is one of them it is a simple, inexpensive, fast method that is easily, produces high-purity nanomaterials and usage in a larger scale for industrial applications.

The overarching goal of this work is to investigate diluted magnetic semiconductors, a class of materials essential in the developing science of spintronics. The existence of magnetic ions impacts the semiconductor characteristics of these materials, both optical and transport. It focuses on fundamental physical mechanisms (such as carrier-ion and ion-ion interactions) and the resultant phenomena. The particular goal of this study is to manufacture Co-doped ZnO nanoparticles with varying concentrations of Co in a dilute ratio using the ball milling method in order to examine the structural, optical, and magnetic characteristics of $Zn_{1-x}Co_xO$ nanoparticles for spintronic devices. This goals were investigated using X-ray diffraction pattern, Scan Electron Microscope (SEM), optical spectrophotometry and magnetometer. Then, interoperating the change in optical and magnetic characterization in terms of the change in nanostructure parameters.

2. Experimental procedures

2.1. Fabrication of ZnO doped Co nanoparticles

Nano-particle powders of $Zn_{1-x}Co_xO$ ($0 \leq x \leq 0.10$) were prepared using ball milling procedure via Fritsch make (Germany) Pulverisette-7 ball mill machine. As the initial step ZnO powder and CoO with 99.999% purity (purchased from Sigma-Aldrich United Kingdom) were combined in the required ratios in a ball mortar and then rotated at an 800 rpm frequency. The combined powders were then sintered in air at 750°C for 5 hrs in order to prevent non-equilibrium phases. Various concentrations of Co ($0 \leq x \leq 0.10$) were prepared to discuss the impact of Co doping on the physical properties of ZnO.

2.2. Characterization

Structural and phases of $Zn_{1-x}Co_xO$ ($0 \leq x \leq 0.10$) nano-particles were investigated via X-ray diffraction (XRD Philips 1710, X'Pert Pro, Panalytical) using Cu Kα radiation (λ=1.540598Å). Besides, the topological characteristics and composition morphology of ZnO pure and doped with Co are determined by the energy dispersion of the X-ray (EDAX) and scanning electron microscope (JEOL JSM-6360LA, Japan),. The absorbance spectra of $Zn_{1-x}Co_xO$ ($0 \leq x \leq 0.10$) nanoparticles analyzed were measured by the Ultraviolet-Visible (UV) absorption spectroscopy (with Shimadzu UV-2101, spectrometer). Finally, the magnetic characteristics of nano-particles were studied utilizing the vibrating sample magnetometer model (VSM model -9600M-1, USA). The measurements have proceeded at temperature equal to 300 K in a maximum applied field of 7 kOe.

3. Results and discussion

3.1. Structural analysis

Fig. 1 (a, b) represents the EDXS spectra of $Zn_{1-x}Co_xO$ with x= 0.05 and x= 0.10 nano-particles respectively,. The spectrum of Co-doped ZnO confirmed the appearance of the peaks identical to Zn, O, and Co. Also, the amount of Co rises with increasing Co ratio in the $Zn_{1-x}Co_xO$ nano-particles system this indicates that the Co ions incorporated successfully into the ZnO lattice.

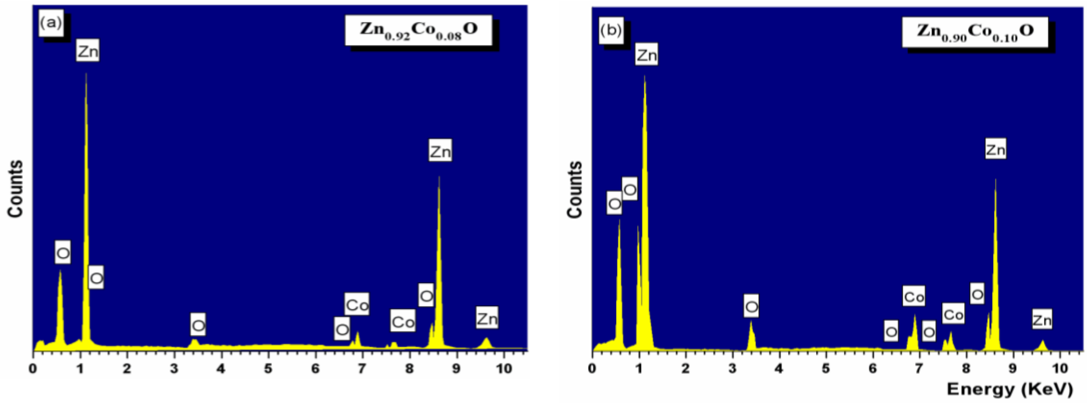

Fig. 1. Energy dispersive x-ray spectra of (a) 8 % and 10 % Co-doped ZnO nanoparticles.

The purity of the ZnO phase was determined by XRD, as seen in the Fig. 2. Using a software X'Pert HighSore, the standard x-ray pattern was simulated referring to Ref. cards Code 01-1136(version 1.0e). The hexagonal wurtzite crystal structure of ZnO was verified by indexing all of the reflection intensities. Furthermore, the time development of XRD peaks of the $Zn_{0.90}Co_{0.10}O$ sample starting from the milled mixture from 2 to 10 hours was depicted in Fig. 3. One can notice that the peaks of CoO (200) and CoO (220) appeared with ZnO peaks for milling period extended from 2 to 6 hour and disappeared at 8 and 10 hours, also, the widening peaks of $Zn_{0.90}Co_{0.10}O$ with rising the milling time owing to a decline in crystal size. There are no CoO peaks identified after 8 and 10 hours of milling time. As a result, the progressive drop in the intensities of CoO peaks with the rise of milling time represents that the Co^{2+} ions progressively enter in the ZnO unit cell substituting the Zn^{2+} ions [21, 27]. No impurity peaks from the tungsten carbide (WC) boat or any other sources are identified up to 10 h milled period. Otherwise, the X-ray patterns can give an effective instrument to investigating the crystalline structure of the Co-doped ZnO. Fig. 4 is demonstrates the crystal structure of $Zn_{1-x}Co_xO$ ($0 \leq x \leq 0.10$) nano-particles up to 10 h milling time. It is noticed that from Fig. 4 the Co-doped ZnO nano-particles exhibits planes of hexagonal wurtzite crystal phase. Simultaneously, the XRD peaks for the doped samples exhibit a substantial shift in the upper 2θ directions 32^o, 35^o, 37^o corresponding to (“100”, “002”, and “101”) in comparison to the un-doped ZnO peak location. This greater shift may be attributed to the inclusion of smaller Co^{2+} ions (0.58 Å) in the hexagonal wurtzite structure, which replaced the Zn^{2+} (0.6 Å). [28, 29]. It demonstrates that, despite the replacement of Co^{2+} ions for Zn^{2+} ions the crystal structure's symmetry stays un-changed, no extraneous peaks observed or other impurities confirming the excellent incorporation of all the elements.

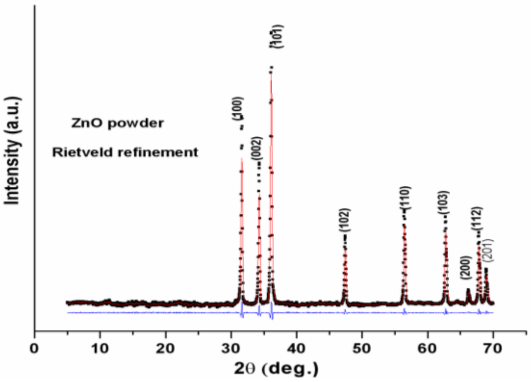

Fig. 2. Rietveld refinement of ZnO powder sample.

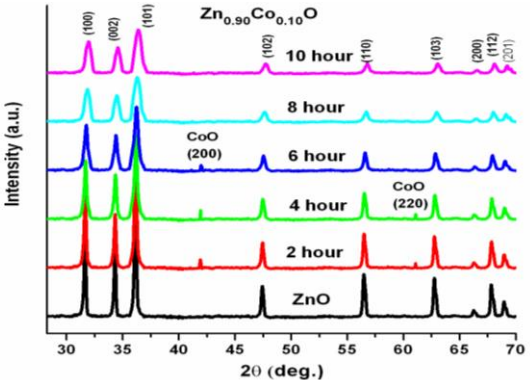

Fig. 3. XRD patterns of $Zn_{0.90}Co_{0.10}O$ *nanoparticles as a function of milling time.*

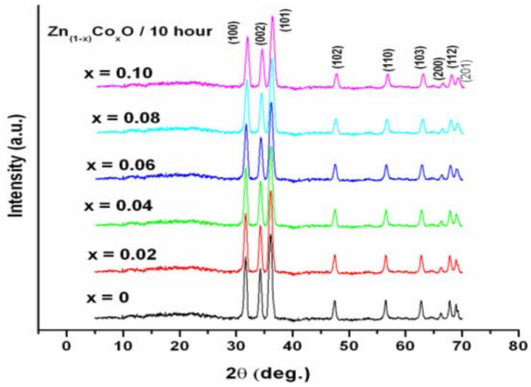

Fig. 4. XRD patterns of $Zn_{0.90}Co_{0.10}O$ *nanoparticles as a function of Co content at milling time 10 hour.*

Moreover, the crystal size "D" for $Zn_{1-x}Co_xO$ ($0 \leq x \leq 0.10$) nano-particles can be determined via Debye Scherrer's equation[30].

$$D = \frac{0.89\lambda}{\beta\cos(\theta)} \tag{1}$$

where λ and β are the wavelength and the full width at half maximum,(FWHM) respectively,. The values obtained for D as a function of ball milling hours increasing and different composition of $Zn_{1-x}Co_xO$ ($0 \leq x \leq 0.10$) nano-particles respectively, was demonstrated in Fig.5. It is obvious that, the crystallite size D reduces as the cobalt incorporation ratio in the ZnO matrix increases. This might be because the replacement of Co^{2+} ions disturbs the ZnO matrix. Consequently cause lattice distortion and subsequent rate of growth [2, 31, 32]. Decreasing trends in crystallite size of Zn1-xCoxO nano-crystals on Co doping have previously been reported[23-25, 33] and interpreted as the suppression of nano-crystal growth owing to Co doping[24, 33]. However, based on Vegard's law higher doping percentages lead to an increase in the volume of the unit cell. The inclusion of Co^{2+} ions into the ZnO matrix could be easily recognized by variations in the lattice constants. It is obvious that, the (F.W.H.M) progressively raises with rising the doping of Co resulting in a reduction in crystal size with Co concentration[23, 34].

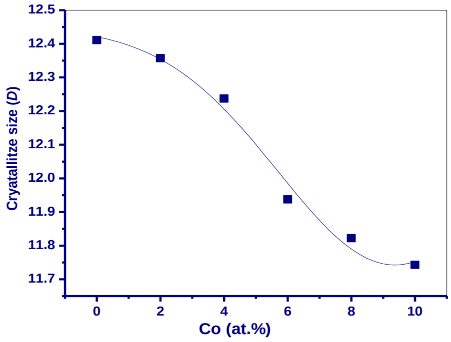

Fig. 5. Dependence of the crystallite size D formed in ZnO nanoparticles as a function of Co% ratio and milling time.

In order to investigate morphology and size of $Zn_{0.92}Co_{0.8}O$ and $Zn_{0.90}Co_{0.1}O$ were used SEM micrographs are noted and explicated in Fig. 6(a and b). The samples display hexagonal structure and alteration in the microstructure with increase Co^{2+} ion doping in ZnO matrix, indicating the replacement of Co ions at the ZnO lattice points[21, 35]. Also, the scans images refer to the nano-particle systems are mostly homogeneous and no possess any sign of Co to accumulate[36].

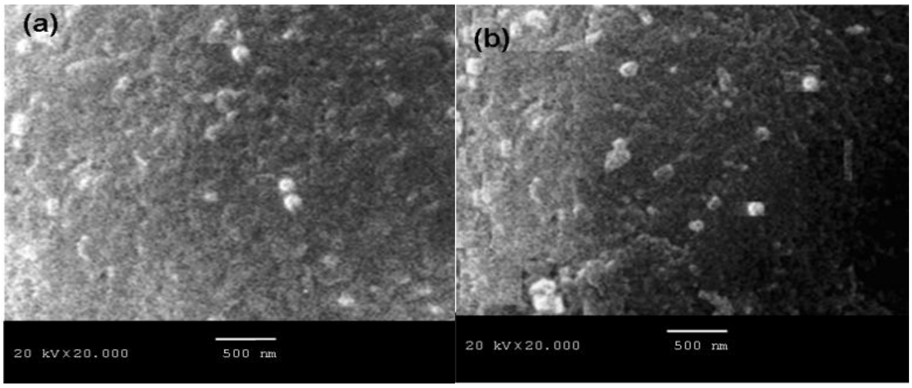

Fig. 6. (a and b). SEM of nanoparticles of (a) $Zn_{0.92}Co_{0.08}O$ and (b) $Zn_{0.90}Co_{0.10}O$.

3.2. Optical characterization

The UV–vis absorption spectra were adopted to measure the absorbance and validate if Zn^{2+} ions are replaced by Co^{2+} ions in Co-doped nano-particle compositions and the variation in bandgap is a serving as a hallmark for this replacement in wavelength range extended from 300 to 1000 nm. Fig.7 illustrates the different composition of $Zn_{1-x}Co_xO$ ($0 \le x \le 0.10$) nano-particles. The spectra of pure ZnO nano-particles clearly shows a sharp edge of ZnO bandgap absorption around 375nm (3.3eV), which is consistent with has been reported in the literature. [37-39]. Moreover, with increased Co the peak has shifted significantly more than in un-doped ZnO, indicating that a considerable number of Co^{2+} ions are present within the ZnO lattice, the optical bandgap was estimated as from ~3.3 eV to 3.22 eV, respectively. Additionally, the redshift of the energy bandgap E_g^{opt} was observed with incorporating Co^{2+} in ZnO [40]. The decrease in the bandgap can be attributed to sp-d replacement interactions which occur between the band and localized electrons of Co^{2+} ions replacing Zn^{2+} ions[40, 41] Otherwise, the spectral of $Zn_{1-x}Co_xO$ nano-particles exhibit three transition peaks with higher Co concentration in the 550 -700 nm region at 565, 610, and 649 nm (Fig. 9), which confirms the replacement of tetrahedral coordinated Co^{2+} ($3d^7$) in ZnO wurtzite structure replacing Zn^{2+} ions are ascribed to the $^4A_2(F)\rightarrow{}^2A_1(G)$, $^4A_2(F)\rightarrow{}^4T_1(P)$ and $^4A_2(F)\rightarrow{}^2E(G)$ dd crystal field transitions[42-44]. The observed transitions in $Zn_{1-x}Co_xO$ nano-particles absorption spectra showed that Co^{2+} ions productively replaced Zn^{2+} within the hexagonal ZnO wurtzite structure.[45, 46].

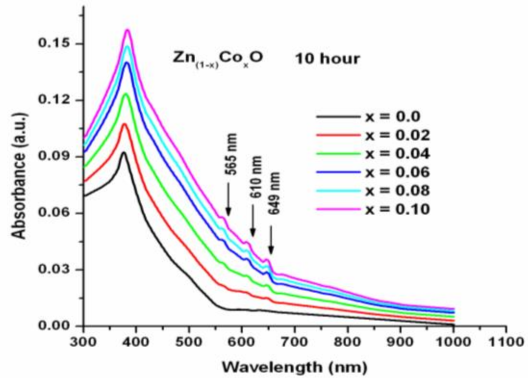

Fig. 7. UV–visible absorption spectroscopy of $Zn_{1-x}Co_xO$ nanoparticle as a function of Co content.

3.3. Magnetic properties

The magnetic characterization of $Zn_{1-x}Co_xO$ (x = 0, 0.02, 0.04, 0.06, 0.08, and 0.10 at.%) nano-particles were investigated at 300 K via utilizing the parallel magnetic fields by a Vibrating Sample Magnetometer (VSM) at RT. Figs. (8 and 9) represent the CoO and un-doped ZnO, reveal a dia-magnetic behavior connected with a ferro-magnetic loop with a visible coercivity and saturation magnetization. The presence of ferro-magnetism(FM) in undoped ZnO materials was reported in literature[47-49]. Sundaresan, A., et al.[50] found that the ferromagnetic origin in non-magnetic oxides such as CoO and un-doped ZnO in RT is linked to un-paired electron spins of oxygen vacancies that exhibit exchange interactions with each other. Furthermore, there is a rise in magnetic moment (emu/g) with an increase in cobalt ratio demonstrated in Fig.10. The variations in the M-H loop can be explained basis on the magnetic contribution from the orientation of the strong exchange interaction in the d-d pair with Co^{+2} ions. A rise of linear behavior of the M-H loop with increase Co doping ratio indicates that the cobalt-cobalt super-exchange prevails with ratio of Co doping at room temperature[51, 52]. however, the existence of intrinsic defects (Zni, OZn, VZn, Oi, etc.) plays a major role in FM interaction in Co doped ZnO systems[53, 54]. Long-range interactions are required to achieve high magnetic FM in dilute Co doped ZnO DMSs, and these can be mediated via defect induced states [55]. According to the bound magnetic polaron (BMP) concept, bound electrons (holes) in defect states can pair with transition metal ions, causing the ferromagnetic areas to overlap, resulting in long range FM ordering[56, 57]. In addition, the magnetic moment of the Co^{2+} can vary depending on the ion environment. The electronic levels splitting and orbital contribution to the cation magnetic moment are determined by the degree of symmetry of the Co site. [58]. Indeed, the symmetry of Co site is accountable about the shape of the bands in the optical absorption spectral this arrangement with the optical spectra as shown in Fig. 9 where the spectral shape variations with the Co ratio.

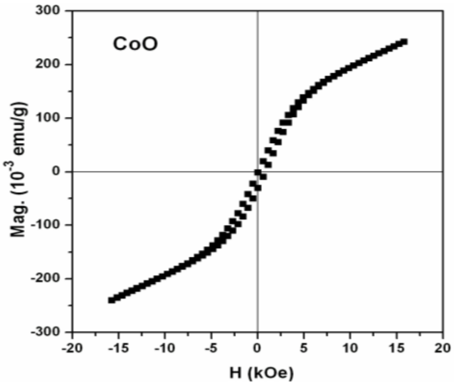

Fig. 8. Variation of magnetization (Mag.) as a function of magnetic field (H) CoO at RT.

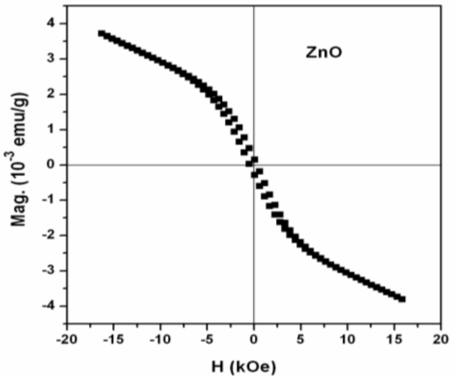

Fig. 9. Variation of magnetization (Mag.) as a function of magnetic field (H) ZnO at RT.

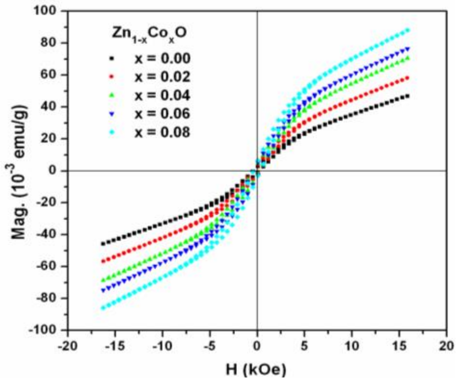

Fig. 10.

Fig. 10. Variation of magnetization (M) as a function of magnetic field (H) of Zn1-xCoxO nanoparticles at (a) 300K.

4. Conclusions

Nano-particles of $Zn_{1-x}Co_xO$ were successfully prepared via ball milling procedure. XRD results exhibit that the doped samples possess growth hexagonal wurtzite crystal phase and significant shift in the higher (“100”, “002” and “101”) planes of the crystal-growth of the examined nano-particles. The optical bandgaps E_g^{opt} of nano-particles $Zn_{1-x}Co_xO$ under studied possess values shifts from ~3.3 eV to 3.22 eV with increasing Co ratio, the variation values of bandgap E_g^{opt} could play an important role for optoelectronic applications. In all nano-particles of

ZnO pure and doped with Co the magnetic measurements showed ferromagnetism (at T = 300 K). The ferromagnetic behavior detected in the ZnO lattice could be ascribed to the substitution of Co^{2+} ions for Zn^{2+} ions. In conclusion, the nano-particles of ZnO could be controlled via optimizing the doping Co% concentration, resulting in intriguing findings for opto-electronic device applications.

Acknowledgements

The authors thank King Khalid University, Ministry of Education, Kingdom of Saudi Arabia for funding this research through a grant: (RCAMS/KKU/013/20) under research center for advanced material science

References

[1] S. Ning, P. Zhan, Q. Xie, W. Wang, Z Zhang, J. Mater. Sci. Technol. **31**, 969 (2015).
[2] M. Nirmala, A. Anukaliani, Physica B: Condensed Matter **406**, 911 (2011).
[3] E. I. Naik, H. B. Naik, M. Sarvajith, E. Pradeepa, Inorganic Chemistry Communications **130**, 108678 (2021).
[4] C. Chai, H. Liu, W. Yu, Chemical Physics Letters **778**, 138765 (2021).
[5] A. F. A. Naim, A. Solieman, E. Shaaban, Journal of Materials Science: Materials in Electronics **31**, 3613 (2020).
[6] D. Bhatia, H. Sharma, R. Meena, V. Palkar, Sensing and bio-sensing research **9**, 45 (2016).
[7] K. Kaviyarasu, G. T. Mola, S. O. Oseni, K. Kanimozhi, C. M. Magdalane, J. Kennedy, M. Maaza, Journal of Materials Science: Materials in Electronics **30**, 158 (2019).
[8] A. A. Alswat, M. B. Ahmad, T. A. Saleh, Colloid and Interface Science Communications **16**, 19 (2017).
[9] G. Poongodi, P. Anandan, R .M. Kumar, R. Jayavel, Spectrochimica Acta Part A: Molecular and Biomolecular Spectroscopy **148**, 243 (2015).
[10] N. P. Shetti, S. J. Malode, D. S. Nayak, G. B. Bagihalli, S. S. Kalanur, R. S. Malladi, C. V. Reddy, T. M. Aminabhavi, K. R. Reddy, Applied Surface Science **496**, 143656 (2019).
[11] M. Alzaid, M. Alwshih, M. N. Abd-el Salam, N. Hadia, Materials Science in Semiconductor Processing **127**, 105687 (2021).
[12] N. S. Kumar, E. H. Al-Ghurabi, M. Asif, M. Boumaza, Sensors and Actuators A: Physical **329**, 112826 (2021).
[13] E.R. Kumar, C. Srinivas, M. S. Seehra, M. Deepty, I. Pradeep, A. S. Kamzin, M. V. K. Mehar, N. K. Mohan, Sensors and Actuators A: Physical **2**, 16 (2018).
[14] H. Nakayama, I. Sakamoto, R. Kinoshita, M. Yasumoto, M. Koike, S. Honda, K. Kuriyama, Japanese Journal of Applied Physics **53**, 05FB03 (2014).
[15] G. Murugadoss, Journal of Materials Science & Technology **28**, 587 (2012).
[16] G. P. Singh, M. K. Roy, Materials Today: Proceedings, (2021).
[17] R. Ahmad, N. Tripathy, Y.-B. Hahn, Chemical Communications **50**, 1890 (2014).
[18] Y. Matsumoto, M. Murakami, T. Shono ,T. Hasegawa, T. Fukumura, M. Kawasaki, P. Ahmet, T. Chikyow, S.-Y. Koshihara, H. Koinuma, Science **291**, 854 (2001).
[19] L. Pereira, M. Nunes, O. Monteiro, A. J. Silvestre, Applied Physics Letters **93**, 222502 (2008).
[19] S. Ogale, R. Choudhary, J. Buban, S. Lofland, S. Shinde, S. Kale, V. Kulkarni, J. Higgins, C. Lanci, J. Simpson, Physical Review Letters **91**, 077205 (2003).
[20] J. Hays, A. Punnoose, R. Baldner, M. H. Engelhard, J. Peloquin, K. Reddy, Physical Review B **72**, 075203 (2005).
[21] I. N. Reddy, C. V. Reddy, M. Sreedhar, J. Shim, M. Cho, D. Kim, Materials Science and Engineering: B **240**, 33 (2019).
[22] S. Ning, P. Zhan, Q. Xie, W. Wang, Z. Zhang, Journal of Materials Science & Technology **31**, 969 (2015).

[23] B. Babu, C.V. Reddy, J. Shim, R. Ravikumar, J. Park, Journal of Materials Science: Materials in Electronics **27**, 5197 (2016).
[24] S. Roy, A.G. Joshi, S. Chatterjee, A. K. Ghosh, Nanoscale **10**, 10664 (2018).
[25] A. Bouaine, N. Brihi, G. Schmerber, C. Ulhaq-Bouillet, S. Colis, A. Dinia, The Journal of Physical Chemistry C **111**, 2924 (2007).
[26] S. Malvankar, S. Doke, R. Gahlaut, E. Martinez-Teran, A. A. El-Gendy, U. Deshpande, S. Mahamuni, Journal of Electronic Materials **49**, 1872 (2020).
[27] A. Salah, A. M. Saad, A. A. Aboud, Optical Materials **113**, 110812 (2021).
[28] A. Fouchet, W. Prellier, P. Padhan, C. Simon, B. Mercey, V. Kulkarni, T. Venkatesan, Journal of applied physics **95**, 7187 (2004).
[29] Y. Fan, Y. Xu, Y. Wang, Y. Sun, Journal of Alloys and Compounds **876**, 160170 (2021).
[30] S. M. Kumaran, R. Gopalakrishnan, Journal of sol-gel science and technology **62**, 193 (2012).
[31] J. Wang, W. Zhou, P. Wu, Journal of nanoparticle research **16**, 1 (2014).
[32] Y. Li, W. Zhou, Y. Yang, P. Wu, Journal of Alloys and Compounds **685**, 448 (2016).
[33] V. Gandhi, R. Ganesan, H. H. Abdulrahman Syedahamed, M. Thaiyan, The Journal of Physical Chemistry C **118**, 9715 (2014).
[34] L. Vegard, Zeitschrift für Physik **5**, 17 (1921).
[35] C. Belkhaoui, N. Mzabi, H. Smaoui, Materials Research Bulletin **11**, 70 (2019)
[36] S. Ghosh, K. Mandal, Journal of Magnetism and Magnetic Materials **322**, 1979 (2010).
[37] M. Bouloudenine, N. Viart, S. Colis, A .Dinia, Chemical Physics Letters **397**, 73 (2004).
[38] M. Bouloudenine, N. Viart, S. Colis, J. Kortus, A. Dinia, Applied Physics Letters **87**, 052501 (2005).
[39] J. H. Kim, H. Kim, D. Kim, Y. E. Ihm, W. K. Choo, Journal of Applied Physics **92**, 6066 (2002).
[40] K. J. Kim, Y. R. Park, Applied Physics Letters **81**, 1420 (2002).
[41] Y. Kim, S. Cooper, M. Klein, B. Jonker, Physical Review B **49**, 1732 (1994).
[42] P. Koidl, Physical Review B **15**, 2493 (1977).
[43] S.-W. Lim, D.-K. Hwang, J.-M. Myoung, Solid state communications **125**, 231 (2003).
[44] N. Srinatha, K. Nair, B. Angadi, Physica B: Condensed Matter **474**, 97 (2015).
[45] J. El Ghoul, M. Kraini, L. El Mir, Journal of Materials Science: Materials in Electronics **26**, 2555 (2015).
[46] A. Simimol, A. A. Anappara, S. Greulich-Weber, P. Chowdhury, H. C. Barshilia, Journal of Applied Physics **117**, 214310 (2015).
[47] S. Zhou, K. Potzger, J. Von Borany, R. Grötzschel, W. Skorupa, M. Helm, J. Fassbender, Physical Review B **77**, 035209 (2008).
[48] L. Xu, K. Shen, Q. Xu, Journal of superconductivity and novel magnetism **24**, 1767 (2011).
[49] S. Zhou, K. Potzger, H. Reuther, K. Kuepper, W .Skorupa, M. Helm, J. Fassbender, Journal of applied physics **101**, 09H109 (2007).
[50] A. Sundaresan, R. Bhargavi, N. Rangarajan, U. Siddesh, C. Rao, Physical Review B **74**, 161306 (2006).
[51] T. Buesgen, M. Hilgendorff, S. Irsen, F. Wilhelm, A. Rogalev, D. Goll, M. Giersig, The Journal of Physical Chemistry C **112**, 2412 (2008).
[52] B. Pal, S. Dhara, P. Giri, D. Sarkar, Journal of alloys and compounds **615**, 378 (2014).
[53] S. Ghosh, G. G. Khan, A. Ghosh, S. Varma, K. Mandal, CrystEngComm. **15**, 7748 (2013) -
[54]J. Liu, S. Lee, Y. Ahn, J.-Y. Park, K. H. Koh, Journal of Physics D: Applied Physics **42**, 095401 (2009).
[55] M. H. Sluiter, Y. Kawazoe, P. Sharma, A. Inoue, A. Raju, C. Rout ,U. Waghmare, Physical review letters **94**, 187204 (2005).
[56] G. McCabe, T. Fries, M. Liu, Y. Shapira, L. Ram-Mohan, R. Kershaw, A. Wold, C. Fau, M .Averous, E. McNiff, Physical Review B **56**, 6673 (1997).
[57] J. M. D. Coey, M. Venkatesan, C. B. Fitzgerald, Nature Materials **4**, 17179-3 (2005).
[58] N. Sakamoto, Journal of the Physical Society of Japan **17**, 99 (1962).